CARTILAGE
2021, Vol. 13(Suppl 2) 336S–345S

DOI: 10.1177/1947603519865320
journals.sagepub.com/home/CAR
SAGE

A 3-Dimensional *In Vitro* Model of Zonally Organized Extracellular Matrix

Sonja M. Walzer[1], Stefan Toegel[1], Catharina Chiari[1], Sebastian Farr[2], Beate Rinner[3], Annelie-Martina Weinberg[4], Daniela Weinmann[1], Michael B. Fischer[5,6], and Reinhard Windhager[1]

Abstract

Objective. Functional cartilage repair requires the new formation of organized hyaline cartilaginous matrix to avoid the generation of fibrous repair tissue. The potential of mesenchymal progenitors was used to assemble a 3-dimensional structure in vitro, reflecting the zonation of collagen matrix in hyaline articular cartilage. *Design*. The 3-dimensional architecture of collagen alignment in pellet cultures of chondroprogenitors (CPs) was assessed with Picrosirius red staining analyzed under polarized light. In parallel assays, the trilineage capability was confirmed by calcium deposition during osteogenesis by alizarin S staining and alkaline phosphatase staining. Using reverse transcription–quantitative polymerase chain reaction (RT-qPCR), mRNA levels of ALP, RUNX2, and BGLAP were assessed after 21 days of osteoinduction. Lipid droplets were stained with oil red O and adipogenic differentiation was confirmed by RT-qPCR analysis of PPARG and LPL gene expression. *Results*. Under conditions promoting the chondrogenic signature in self-assembling constructs, CPs formed an aligned extracellular matrix, positive for glycosaminoglycans and collagen type II, showing developing zonation of birefringent collagen fibers along the cross section of pellets, which reflect the distribution of collagen fibers in hyaline cartilage. Induced osteogenic and adipogenic differentiation confirmed the trilineage potential of CPs. *Conclusion*. This model promotes the differentiation and self-organization of postnatal chondroprogenitors, resulting in the formation of zonally organized engineered hyaline cartilage comparable to the 3 zones of native cartilage.

Keywords

extracellular matrix, tissue, polarized light microscopy, research methods, chondrogenesis, cells

Introduction

Zonal organization of extracellular matrix (ECM) plays an important role in hyaline cartilage structure and maintenance of cartilage functionality. In articular joints, cartilage integrity is mainly responsible for patients' mobility and activity. Injuries or degenerative changes often cause cartilage lesions, which are unfortunately limited in terms of self-healing because of the cartilaginous avascular structure, low cellularity, and minor ECM formation capability. Therefore, *in vivo* restoration and *in vitro* reconstruction of zonally organized hyaline cartilage is the goal of numerous tissue engineering approaches.[1-3] So far, engineered tissues turned out to be hardly comparable to hyaline cartilage and its zonal organization.[4] For this reason, the search for the optimum cell source[5-7] density[8] and suitable biomaterials[4,9-11] for zonal organization in hyaline cartilage repair or engineered tissue is still ongoing.[12-17] Recently, Zhu *et al*[4] presented artificially produced zonal hydrogels for organized tissue repair and imitated zonal-specific cartilage, verified by the expression of collagen II, glycosaminoglycans, and collagen X in encapsulated bovine chondrocytes and mesenchymal stem cells (MSCs). However, the different approaches in using cells of the mesenchymal lineage—including MSCs or chondrocyte precursors—for cell-based hyaline cartilage repair, have so far resulted in merely

[1]Karl Chiari Lab for Orthopaedic Biology, Department of Orthopedics and Trauma Surgery, Medical University of Vienna, Vienna, Austria
[2]Orthopaedic Hospital Speising, Vienna, Austria
[3]Division of Biomedical Research, Medical University of Graz, Graz, Steiermark, Austria
[4]Department of Orthopaedic and Trauma Surgery, Medical University of Graz, Graz, Steiermark, Austria
[5]Center for Biomedical Technology, Danube University Krems, Krems an der Donau, Austria
[6]Clinic for Bloodgroup Serology and Transfusion Medicine, Medical University of Vienna, Vienna, Austria

Supplementary material for this article is available on the *Cartilage* website at https://journals.sagepub.com/home/CAR.

Corresponding Author:
Sonja M. Walzer, Karl Chiari Lab for Orthopaedic Biology, Department of Orthopedics and Trauma Surgery, Medical University of Vienna, Waehringer Guertel 18-20, Vienna, 1090, Austria.
Email: sonja.walzer@meduniwien.ac.at

randomly aligned matrix assembly[18-20] as demonstrated in histological evaluation of the newly formed tissue.

Because of their ability for migration and differentiation, endogenous stem cells of the mesenchymal lineage resident in growth plate tissue could represent a promising cell source to study hyaline cartilage repair.[19] In this context, transplantation of *in vitro* expanded epiphyseal cells in a scaffold-based fracture healing small animal model resulted in increased bone density on the fracture side while disorganized tissue repair was found in the untreated mice.[21] At low passages, epiphyseal cells implanted in the back skin of 6- to 8-week-old mice formed cartilage-like tissue without ossification, whereas tissue formed by cells of higher passages was absorbed and could therefore not be preserved over a longer period.[22] Recently, we showed that human chondroprogenitors (CPs) can be isolated from polydactyl digits,[23] characterized by MSC-related surface markers and cultured with mechanical stimulation and pro-inflammatory conditions in monolayer cultures,[24] although the hyaline cartilage formation of human CPs *in vitro* remained largely unknown. In particular, the ability of CPs to differentiate into the 3 mesenchymal linages is expected to decisively affect the formation of repaired tissue and de novo synthesized hyaline extracellular matrix.

The present study extends previous observations by investigating the potential of human CPs to promote the chondrocyte phenotype in 3-dimensional (3D) constructs associated with the organization of cells and the autologous assembly of cartilaginous matrix. In addition—to confirm the trilineage potential of these cells—we programmed CPs to differentiate into adipogenic and osteogenic lineages in monolayer culture systems.

Materials and Methods

Growth plate (GP)-CP Cell Isolation and Cell Expansion

Clinical specimens of the human GP were obtained from the supernumerary digits of 8 different donors (age <36 months) with polydactylism at the time of surgical excision. Specimens were collected with informed consent of the donors' parents and in full compliance with the terms of the Ethics Committee of the Medical University of Graz (20-344ex 08/09) and the Ethics Committee of the Medical University of Vienna (EK Nr.: 1830/2012). Only cartilaginous components without ossification centers were included in the study. Growth plate tissue was digested using 2 mg/mL Collagenase B (Roche Diagnostics) as previously reported[18,19] and plated in α-MEM supplemented with 10% fetal bovine serum (FBS), 2% penicillin-streptomycin 0.5% L-glutamine (all GIBCO Invitrogen), 0.2% amphothericine B (PAA Laboratory, GE Healthcare), in 75 cm^2 culture flasks in a humidified atmosphere with 5% CO_2 at 37°C. When reaching 80% to 90% confluence, cells were subjected to fluorescence-activated cell sorting (FACS) as previously described.[24] Briefly, 1 × 10^6 cells/mL were incubated for 1 hour at 4°C with 5 µg/mL of primary conjugate antibodies specific for CD45−, CD34−, CD73+, CD90+, CD105+ (BD Bioscience) as previously described by our group.[19,20] Nonviable cells were stained with 1 µg/mL of propidium iodide (Molecular Probes, Eugene, OR) and excluded from the analysis. To set background fluorescence levels, unstained and/or matched isotype controls were used. For all ensuing experiments of this study, cells were used at passages 0 to 2.

Three-Dimensional Constructs

To promote chondrogenesis, 5 × 10^5 cells were centrifuged at 150 g for 10 minutes in V-shaped tubes (Eppendorf) for each pellet (n = 3 donors) and cultured at 37°C with 5% humidity in 500 µL DMEM–low glucose (Gibco) containing 10 µg/mL ITS (Roche), 1% gentamycin, 10 ng/mL TGF-β1 (R&D), and 50 ng/mL ascorbic acid for up to 5 weeks.

Histology and Histochemistry

Cell pellets were harvested, fixed with neutral-buffered 7.5% formaldehyde (Merck) for 10 minutes and embedded in paraffin. From each pellet, the midsagittal 2.5-µm sections were processed for toluidine blue (TB) and Alcian blue staining to evaluate glycosaminoglycans in the ECM.[25] Picrosirius red (PSR) staining was conducted on cell pellets and articular cartilage tissue samples for collagen determination under light microscopy (LM) and polarized light microscopy (PLM, Zeiss Oberkochen, Germany). Images of sections of CP pellets stained with PSR were converted into grayscale images.[26] Collagen alignment in the images was investigated in 10 representative independent regions of interest (ROI) in the superficial, middle and deep zone. The digitized gray shade images were analyzed with Photoshop software using a reported semiquantitative analysis of ECM in articular cartilage. The total pixel number of 300 × 300 was kept constant in all selected ROIs. The optical density plot was generated by the histogram tool in 10 ROIs in each zone. The mean signal intensity (arbitrary units, AU) in each ROI was recorded as a measure for the signal intensity of the oriented collagen fibrils.

Immunofluorescence Detection of Collagen Type II

Deparaffinized sections were blocked with 10% donkey serum (Jackson Immunotech) for 30 minutes and incubated with 2.5 µg/mL mouse anti-collagen II antibody (OriGene–Acris Antibodies US) in 0.05 M tris(hydroxymethyl)-aminomethane buffer overnight. After washing the slides with tris-buffered saline (TBS) 2 times, 2 µg/mL Alexa Fluor (AF)-555 conjugated donkey anti-mouse Ab (Life

Technologies Invitrogen) were added for 1 hour. Cell nuclei were counterstained with DAPI (Sigma). Isotype controls were included in the protocol and were immunonegative throughout the experiments. Images were created on an LSM 700 confocal laser scanning microscope (Carl Zeiss, Germany) equipped with ZEN black imaging software.

In Vitro *Osteogenic and Adipogenic Differentiation*

CPs were seeded at a density of 10^4 cells/cm^2 in DMEM–low glucose (GIBCO) containing 10% FBS (Lonza), 1% penicillin-streptomycin, 1% L-glutamine, and 0.1% amphotericine B. For the induction of osteogenic differentiation, the medium was supplemented with 10 nM dexamethasone, 0.1 mM ascorbic acid-2-phosphate, and 10 mM β-glycerophosphate (all from Sigma). Alkaline phosphatase (ALP) activity was assayed at days 7 and 14 by biochemical staining (Alkaline Phosphatase kit No. 85, Sigma) following the manufacturer's instructions. ALP enzyme activity was calculated after measuring the absorbance of *p*-nitrophenol phosphate product at 405 nm using a microplate reader (BioRad). For the alizarin red S (ARS) staining of calcium deposits, cells were fixed with 10% formaldehyde (Merck) at days 7, 14, and 21 and incubated with 1% ARS staining solution (Sigma). Quantitation of ARS staining was performed by elution of the fixed cells with 10% cetylpyridium chloride (Sigma) prior to measuring the absorbance at 570 nm on a microplate reader. For adipogenic induction, the medium was supplemented with 0.1 μM dexamethasone, 50 μM indomethacine (both from Sigma) and 5 μg/mL insulin (Novo Nordisk). Fat vacuoles were stained with oil red O (Sigma) on day 21 as previously reported.[25]

Reverse Transcription–Quantitative Polymerase Chain Reaction

Twenty-one days after adipo- and osteoinduction, total RNA ($n = 4$ donors) was extracted using the RNeasy kit (Qiagen) according to the manufacturer's instructions. Each sample was run on the Agilent 2100 Bioanalyzer Nano LabChip for quality control and quantification of total RNA prior to reverse transcription into cDNA using the high-capacity cDNA reverse transcription kit (Applied Biosystems). RNA integrity numbers were between 9.3 and 10. The reverse transcription–quantitative polymerase chain reactions (RT-qPCRs) were performed on an Applied Biosystems StepOnePlus qPCR device using SYBR Green PCR Master Mix (Life Technologies), sequence specific primers for HRPT1 (Fwd: TGACACTGGCAAAACAATGCA; Rev: GGTCCTTTTCACCAGCAAGCT), GAPDH (Fwd: GGAGTCCACTGGCGTCTTCAC; Rev: GAGGCATTGC TGATGATCTTGAGG), ALP (Fwd: TGATGTGG AGTATGAGAGTGAC; Rev: TGAAGTGGGAGTGCTT GTATC), RUNX2 (Fwd: CTTGTGGCTGTTGTGATGC; Rev: CTGTTGCTGCTGCTGTTG), BGLAP (Fwd: GCAG AGTCCAGCAAAGGTG; Rev: CCAGCCATTGATACA GGTAGC), LPL (Fwd: GACACTTGCCACCTCATTCC; Rev: ACTCTCATACATTCCTGTTACCG), and PPARG (Fwd: ACGAAGACATTCCATTCACAAG; Rev: CAGGCTCCACTTTGATTGC) at a concentration of 100 nM, and 1 μL cDNA (diluted 1:5) under the following conditions: 95°C for 10 minutes followed by 40 cycles of 15 seconds of denaturation at 95°C, 60 seconds of annealing at 55°C and 60 seconds of elongation at 72°C. A melting curve analysis was performed after each run to confirm product specificity. mRNA expression levels were calculated as relative copy numbers considering actual amplification efficiencies. Technically, the protocol deliberately followed the minimal guidelines for the design and documentation of RT-qPCR experiments (MIQE) as recently outlined.[27,28]

Statistical Analyses

Data were exported to Graph Pad Prism 5 and SPSS for analysis. Results were expressed as mean ± SD. Normal distribution of data was assessed using Shapiro-Wilk test. Paired *t* test was used to test the difference between groups for parametric data and Mann-Whitney *U* was used for nonparametric data. Statistical significance was set at a level of $P < 0.05$.

Results

ECM Organization in 3D Constructs of CPs

Self-assembling pellet cultures were used to promote the chondrogenic phenotype of CPs after expansion in monolayer culture (**Fig. 1A**). To investigate the accumulation of extracellular matrix components, we performed histological analyses showing an augmented amount of glycosaminoglycans, as visualized by Alcian blue staining after 21 days and cartilage-specific metachromasia shown in TB staining (**Fig. 1B**). In the cartilaginous matrix, the cells begin to self-organize in column like formations. Expression of the cartilaginous marker collagen type II and superficial appearance of collagen type I in the cell construct in superficial (**Fig. 2A**) and central (**Fig. 2B**) areas was detected after 21 days by immunofluorescence. Collagen type II positivity was detected in the newly formed ECM around the center of the pellet (high cell density), whereas collagen type I imunostaining was mainly found in the superficial zone, with weak positivity in the central area of the CP pellet.

The 3D architecture of the collagen structure in human CP pellets was studied by PSR staining and PLM after 5 weeks of cultivation (**Fig. 3A**). The different arrangement of birefringent collagen fibers along the cross-section of the pellets indicated developing zonation in the newly formed

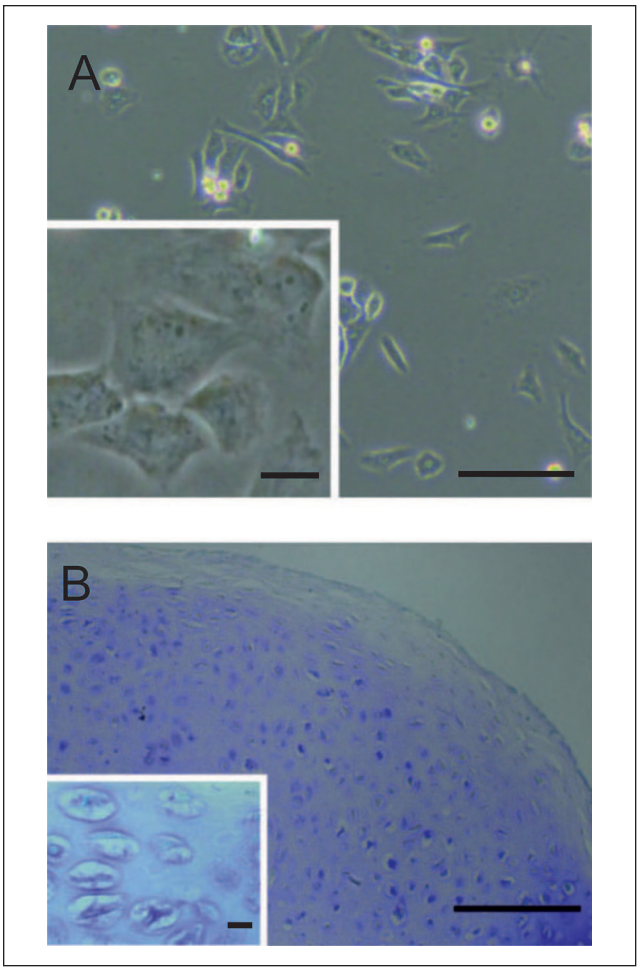

Figure 1. (**A**) Morphology of isolated chondroprogenitors (CPs) in 2-dimensional culture (200× magnification). (**B**) Image of toluidine blue staining of self-organization of cells in column-like formations in the newly formed extracellular matrix (ECM) in 3-dimensional pellets (200× magnification, light microscopy). Scale bar equals 50 µm.

hyaline matrix. Parallel to the pellet surface (PS), horizontally arranged birefringent fibers were mainly found in the margin of the pellet (**Fig. 3A**). Randomly organized collagen fibers formed the central area of the cartilaginous matrix (**Fig. 3B**). Perpendicularly oriented birefringent fibers (**Fig. 3C**) occurred in major parts of the collagen matrix in proximity to the cell-condensed center. Visualizing the collagen alignment in equally processed native articular cartilage, the architecture of the matrix indicated a comparable pattern (**Fig. 4**). Birefringent collagen fibers in the superficial zone (A) were parallel orientated to the articular surface. Randomly organized fibers were found in the middle (B) and perpendicularly oriented leaf-like arcades in the deep (C) zone. Additionally, a semiquantitative analysis of the developed zonation was performed under PLM in pellets and cartilage tissue, where increased signal was associated with increased collagen fibril assembly in the ECM. In the superficial zone (**Fig. 5 left**) and in the middle zone (**Fig. 5 middle**) no significant differences between signals obtained in GP-CP pellets and cartilage specimens were detected. ROIs in the deep zone (**Fig. 5 right**) of articular cartilage yielded the strongest staining. The mean staining intensities (±SD) underlying the plots depicted in **Figure 3B** are additionally presented in Supplementary Tables S1 and S2 (available online).

Osteogenic Differentiation of GP-CPs

Biochemical quantitation of ALP staining significantly increased at days 7 and day 14 compared with the undifferentiated control ($n = 8$, $P < 0.001$). ARS quantitation revealed a significant increase of calcium deposits during osteoinduction in CPs over time ($n = 8$, $P < 0.001$) when compared with undifferentiated controls (**Fig. 6A**). In agreement, mRNA levels of ALP, a marker for early osteogenesis, and BGLAP, a marker of late osteogenesis, were increased 20.9 ± 25.2- and 6.7 ± 4.69-fold, respectively, while those for transcription factor RUNX2 were significantly upregulated 2.88 ± 1.04-fold, supporting the osteoinduction of GP-CPs. Supporting lineage identity, osteoinductive conditions did not alter the expression of the adipocyte-related gene PPARG, and induced LPL mRNA levels only to a minor (1.24 ± 0.6-fold), albeit statistically significant, extent (**Fig. 6B**).

Adipogenic Differentiation of GP-CPs

The capability of CPs for adipogenic differentiation was demonstrated by oil red O staining of lipid droplets, first appearing intracellularly after 7 days postinduction and covering diffuse areas in the monolayer after 21 days (**Fig. 7A**). In contrast, lipid droplets were absent after 21 days of culture in the undifferentiated control group (**Fig. 4C**). mRNA levels of early (PPARG) and late (LPL) adipogenic markers were assessed at day 21 (**Fig. 7B**), showing that PPARG levels were significantly upregulated (2.0 ± 0.6-fold; $P < 0.05$), whereas LPL was strongly, but not significantly, upregulated (1054.44 ± 906.61-fold) due to the high degree of interindividual variability across the individual donors. Under the adipogenic program, ALP was not significantly increased whereas RUNX2 was significantly decreased (**Fig. 4D**).

Discussion

In our present study, the *in vitro* condensation of CPs in pellet cultures led to cartilaginous ECM formation, reflecting the collagen alignment in native hyaline cartilage. To the best of our knowledge, we are not aware of any study in the literature where collagen fiber zonation of epiphyseal CPs was shown

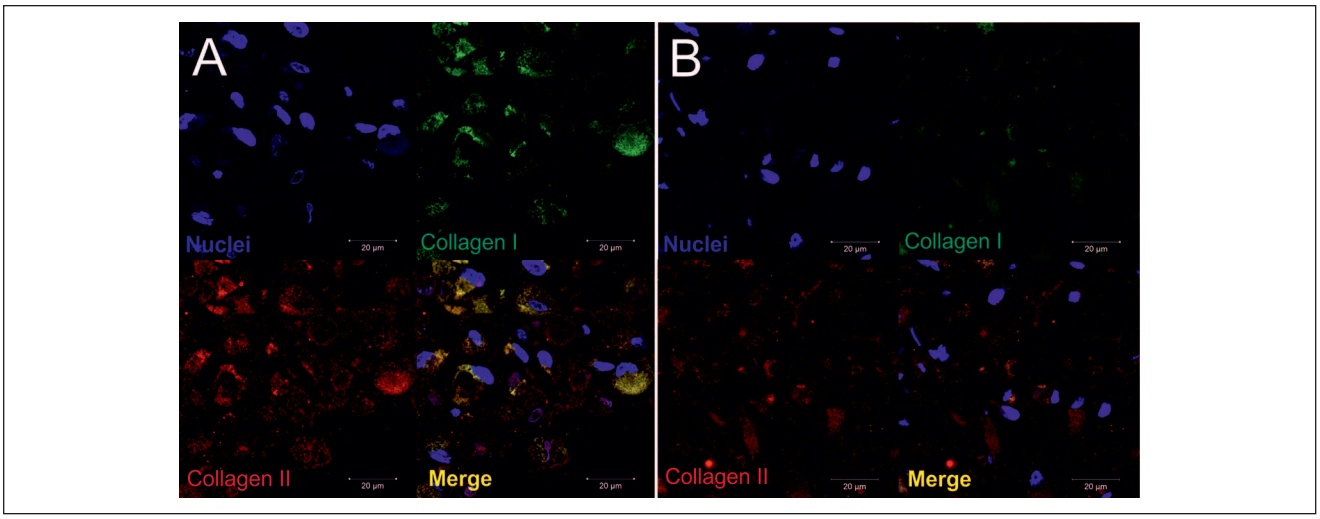

Figure 2. Immunopositivity for collagen I and collagen II in (**A**) superficial and (**B**) central regions of the chondroprogenitor (CP) pellet, visualized by confocal laser microscopy at 630× magnification. Nuclei were stained with DAPI (4′,6-diamidino-2-phenylindole) (blue).

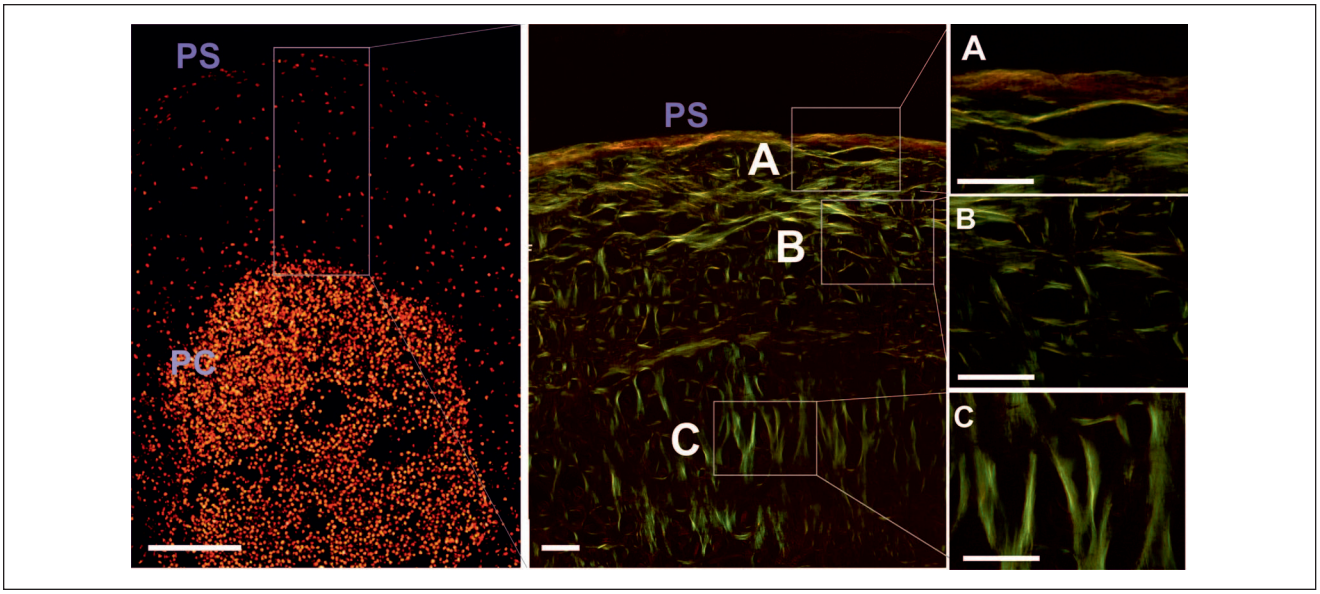

Figure 3. Representative images of cell distribution and fiber orientation in the collagen matrix in chondroprogenitor (CP) pellets. Birefringent collagen fibers show developing zonation in the newly formed hyaline matrix and parallel to the pellet surface (PS) horizontal arranged birefringent fibers in the margin (**A**). Randomly organized collagen fibers were found in the central area (**B**). Perpendicularly oriented birefringent fibers (**C**) were located in proximity to the cell condensed center. Scale bar equals 30 µm, 400× magnification.

in perpendicular orientation to the pellet surface. Murdoch *et al*.[29] showed some bright fibrils radiating from the pellet center in pellet cultures of hMSCs undergoing chondrogenic differentiation. The qualitative evaluation of collagen fibre orientation and potential zonation is often neglected in culture systems without scaffolds or matrices like pellet cultures. We therefore focused in our study on the birefingence of the collagen fibers in the newly formed cartilaginous ECM of human CPs after cell condensation in 3D pellet cultures. Photoshop-based analysis was previously used in articular cartilage tissue for different histological and immunohistological stainings by Lahm *et al*.[26] In our study, we implemented this method for the analysis of the collagen alignment in PSR images and show that the collagen orientation in the

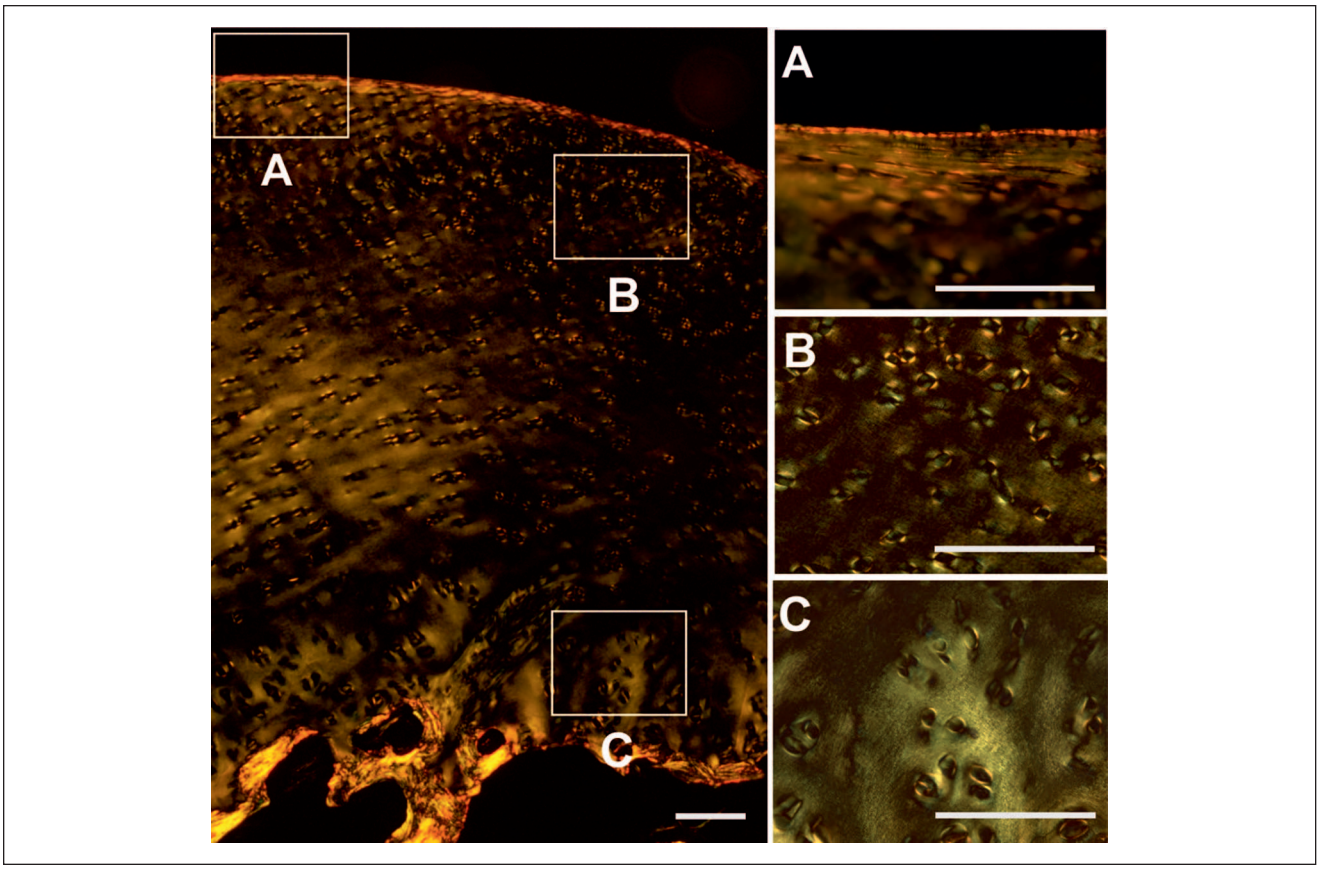

Figure 4. For comparison, images of articular cartilage tissue show birefringence of collagen fibers in the superficial (**A**), middle (**B**), and deep (**C**) zone in human articular cartilage tissue. Scale bar equals 100 µm, 200× magnification.

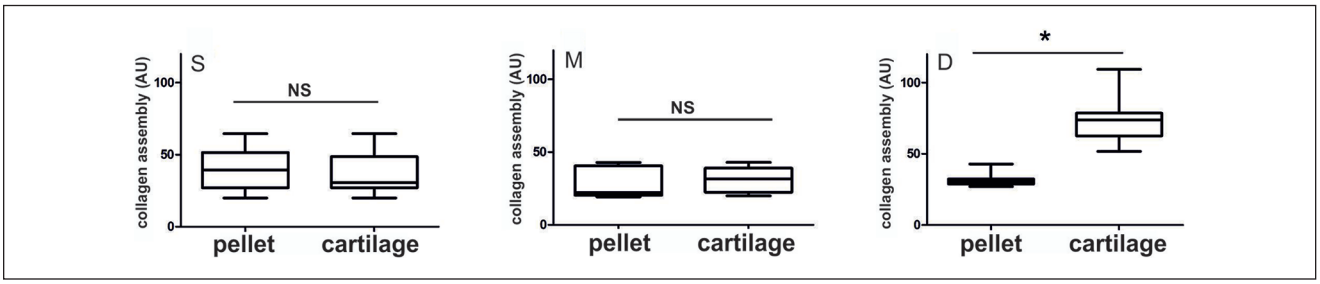

Figure 5. Grayscale analysis showed no significant difference between the zonation in the newly formed hyaline cartilage in chondroprogenitor (CP) pellets and zonal distribution in the superficial (depicted as S) and middle (depicted as M) areas compared with cartilage tissue. For the perpendicularly oriented birefringent arcades (depicted as D), a significant difference between CP pellets and articular cartilage tissue was detected (*$P < 0.05$).

newly formed matrix in the superficial and the middle zones of CP pellets matched with the collagen orientation in the equivalent zones of articular cartilage tissue. The perpendicularly oriented collagen fibers in the CP pellets around the cell condensed center qualitatively reflected the collagen orientation in the deep zone of articular cartilage, however, within the time of cultivation the newly formed arcades did not yet reach the prominence of the arcades in native tissue. To investigate line identity and trilineage potential, adipogenic and osteogenic differentiation in CP monolayer cultures could be verified by the expression of lineage specific markers at the gene and protein level. Given their remarkable potential for differentiation and collagen fiber organization in the newly formed hyaline cartilage, CPs might therefore represent an interesting cell source to unravel the mechanisms involved in cellular programmability and self-organization.

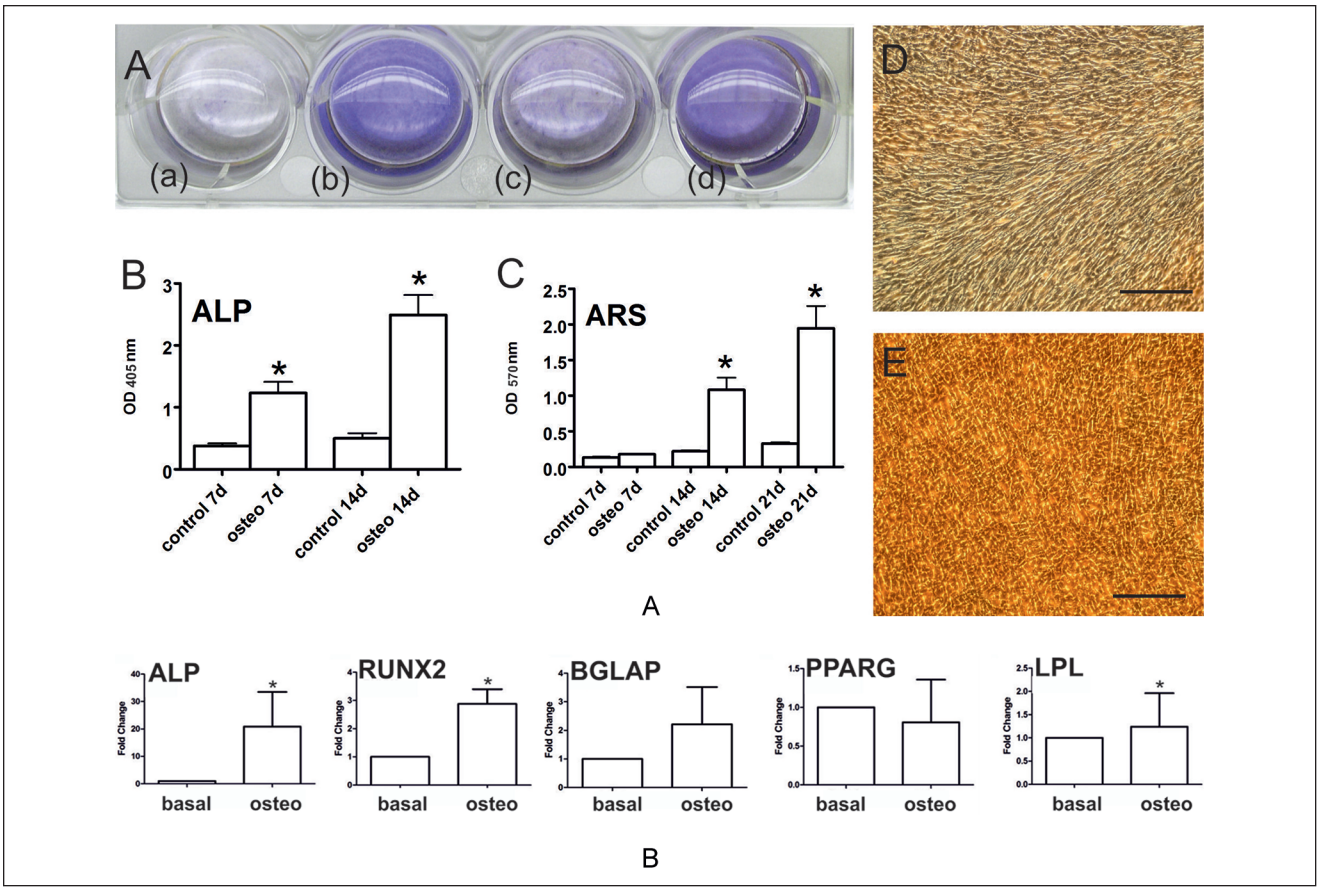

Figure 6. (**A**) Alkaline phosphatase (ALP) (*$P < 0.001$; $n = 8$; OD 405 nm) and alizarin red S (ARS; *$P < 0.001$; $n = 8$; OD 405 nm) staining verified increased osteoinduction after 7 days (**b**) and 14 days (**d**) compared with the appropriate undifferentiated control (**a**, **c**). (**B**) Osteogenic differentiation of GP-CPs showed increased expression on mRNA levels of early osteogenic gene ALP and a significant upregulation of transcription factor RUNX2 compared with basal levels (*$P < 0.05$; $n = 4$). BGLAP as a marker of late osteogenesis was increased compared to the undifferentiated control. Osteogenic programmed GP-CPs showed nonsignificant modulation of the adipocyte-related gene PPARG and minor upregulation at low levels of LPL. Images show ARS staining of untreated (**D**) and osteogenic (**E**) differentiated cells of one representative sample after 21 days. Scale bar equals 200 µm.

The zonally aligned collagen network of healthy hyaline cartilage—characterized by leaf-like-arcades—confers maximal load-bearing properties to the tissue.[30] Thus, cartilage regeneration aims at restoring the correct assembly and alignment of collagens and other ECM molecules to fulfill the mechanical requirements for functional tissue repair.[1] It is well known, however, that current cartilage repair strategies including microfracturing and other cell-based therapies often fail at functional tissue regeneration or integration. On one hand, cells are the main players in the process of matrix remodeling, while, on the other hand, an aligned matrix provides structural and signaling cues to guide cell fate decision.[31] Interestingly, recent laboratory work highlighted that ECM proteins, presented to cells in a 3D environment, are potent triggers of MSC differentiation into all lineages.[16] Consequently, ECM-cell interaction and associated signal transduction pathways—as well as differentiation programs that are initiated by these interactions—may be closely related to functional tissue regeneration. One factor that may influence the orientation of chondroprogenitor cells in the newly formed tissue is the primary cilium, which is also modulated during the cellular repair program.[31] In MSCs, the primary cilium is important to maintain the differentiation program and continue lineage commitment during the differentiation process.[32] Intraflaggellar transport proteins (IFT 80 and IFT 88) as well as IFT motorproteins (KIF3A) and primary cilia proteins are also involved in chondrocyte differentiation.[33] In transgenic mice (Col2aCre;Ift88(fl/fl)), in which primary cilia were deleted in chondrocytes, the thickness and the mechanical properties of cartilage—especially in the deeper zones—was reduced.[34] Since our study showed the spontaneous perpendicular arrangement of collagen fibers in the "deep zone" of CP pellets, upcoming studies using the presented model will contribute to investigate the involvement of ciliary-related proteins in the aligned formation of newly formed ECM.

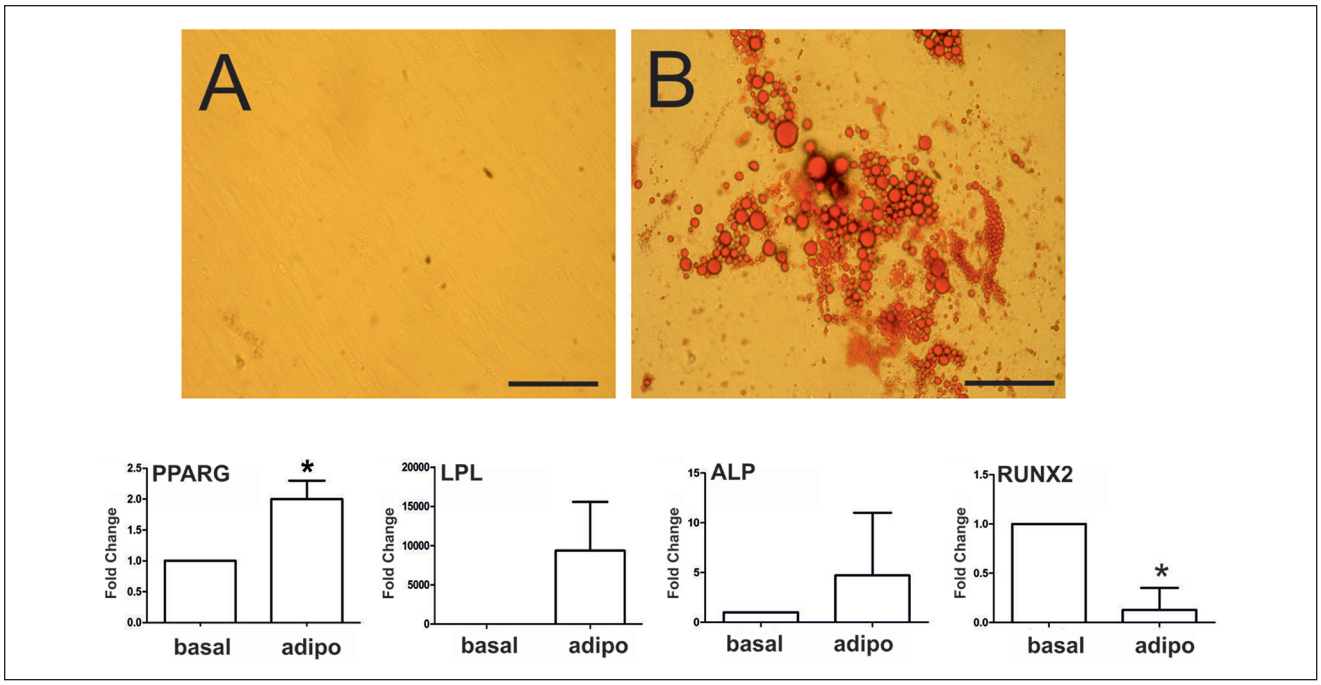

Figure 7. (**A**) *In vitro* adipogenic differentiation of GP-CPs in 2-dimensional cultures. Oil red O staining of intracellular heterogeneous lipid vacuoles in Growth plate – cultures of chondroprogenitors (GP-CPs) without and after adipoinduction. Scale bar equals 100 µm. (**B**) Assessment of early and late adipogenic genes revealed significantly increased expression of PPARG and highly increased LPL expression compared with basal levels. Under the adipogenic program, ALP levels were not significantly altered, whereas RUNX2 was significantly downregulated (*$P < 0.05$; $n = 4$).

Three-dimensional pellets have several advantages over 2D monolayer cultures, for example regarding the elevated expression of matrix proteins such as collagen II. However, the 3D pellet cultures have limitations in the output of chondrogenesis and to be directly transferred to tissue engineering applications. To overcome the limitations of culturing CPs in pellets, the next steps will involve the culturing of human epiphyseal–derived CPs in hydrogels/matrices and transport the system into an in situ setting in a sheet like structure. *In situ* culturing will allow to develop the newly formed matrix over a longer period of time or to apply mechanical testing or perform µMRI of the newly formed matrix. In addition, these approaches could then be compared to histological information on the orientation of the newly formed collagen fiber network, analyzed using qPLM.

Conclusions

To our knowledge, the present report is first to show zonally organized hyaline matrix in a model of in vitro cartilage formation where the newly assembled matrix reflects the organization of its physiological template. CPs hold a trilineage potential by differentiating also into osteoblasts and adipocytes during induced differentiation programs. Although being a rare cell source, CPs might represent a model for self-organization in functional tissue regeneration or engineering approaches involving programmed cells and aligned matrices in the future.

Acknowledgments and Funding

Bettina Rodriguez Molina, Ruth Grübl Barabas, Melanie Cezanne, Melanie Schmid, and Heike Kaltenegger are gratefully acknowledged for excellent technical assistance. The author(s) received no financial support for the research, authorship, and/or publication of this article.

Declaration of Conflicting Interests

The author(s) declared no potential conflicts of interest with respect to the research, authorship, and/or publication of this article.

Ethical Approval

Specimens were collected in full compliance with the terms of the Ethics Committee of the Medical University of Graz (20-344ex 08/09) and the Ethics Committee of the Medical University of Vienna (EK Nr. 1830/2012).

Informed Consent

Specimens were collected with informed consent of the donors' parents.

Trial Registration

Not applicable.

ORCID iD

Sonja M. Walzer https://orcid.org/0000-0002-9056-4330

Supplemental Material

The supplementary material for this article is available online.

References

1. Ahmed TA, Hincke MT. Strategies for articular cartilage lesion repair and functional restoration. Tissue Eng Part B Rev. 2010;16(3):305-29.
2. Hughes L, Archer C, Ap Gwynn I. The ultrastructure of mouse articular cartilage: collagen orientation and implications for tissue functionality. A polarised light and scanning electron microscope study and review. Eur Cell Mater. 2005;9:68-84.
3. Chen FH, Tuan RS. Mesenchymal stem cells in arthritic diseases. Arthritis Res Ther. 2008;10(5):223.
4. Zhu D, Tong X, Trinh P, Yang F. Mimicking cartilage tissue zonal organization by engineering tissue-scale gradient hydrogels as 3D cell niche. Tissue Eng Part A. 2018;24(1-2):1-10.
5. O'Sullivan J, D'Arcy S, Barry FP, Murphy J, Coleman CM. Mesenchymal chondroprogenitor cell origin and therapeutic potential. Stem Cell Res Ther. 2011;2(1):8.
6. Taipaleenmäki H, Suomi S, Hentunen T, Laitala-Leinonen T, Säämänen AM. Impact of stromal cell composition on BMP-induced chondrogenic differentiation of mouse bone marrow derived mesenchymal cells. Exp Cell Res. 2008;314:2400-10.
7. Davies BM, Snelling SJ, Quek L, Hakimi O, Ye H, Carr A, *et al*. Identifying the optimum source of mesenchymal stem cells for use in knee surgery. J Orthop Res. 2017;35(9):1868-75.
8. Wiliams CG, Klein TJ, Sah RL. Cell density alters matrix-accumulation in two distinct fractions and the mechanical integrity of alginate-chondrocyte constructs. Acta Biomater. 2003;1:625-33.
9. Mellati A, Fan CM, Tamayol A, Annabi N, Dai S, Bi J, *et al*. Microengineered 3D cell-laden thermoresponsive hydrogels for mimicking cell morphology and orientation in cartilage tissue engineering. Biotechnol Bioeng. 2017;114(1):217-31.
10. Mellati A, Dai S, Bi J, Jin B, Zhang H. A biodegradable thermosensitive hydrogel with tuneable properties for mimicking three-dimensional microenvironments of stem cells. RSC Adv. 2014;4(109):63951-61.
11. Nuernberger S, Cyran N, Albrecht C, Redl H, Vécsei V, Marlovits S. The influence of scaffold architecture on chondrocyte distribution and behavior in matrix-associated chondrocyte transplantation grafts. Biomaterials. 2011;32(4):1032-40.
12. Zeiger AS, Loe FC, Li R, Raghunath M, Van Vliet KJ. Macromolecular crowding directs extracellular matrix organization and mesenchymal stem cell behavior. PloS One. 2012;7(5):e37904.
13. Saeidi N, Sander EA, Ruberti JW. Dynamic shear-influenced collagen self-assembly. Biomaterials. 2009;30(34):6581-92.
14. Shirazi R, Shirazi-Adl A, Hurtig M. Role of cartilage collagen fibrils networks in knee joint biomechanics under compression. J Biomech. 2008;41(16):3340-8.
15. Shirazi R1, Shirazi-Adl A. Deep vertical collagen fibrils play a significant role in mechanics of articular cartilage. J Orthop Res. 2008;26(5):608-15.
16. Jung JP, Bache-Wiig MK, Provenzano PP, Ogle BM. Heterogeneous differentiation of human mesenchymal stem cells in 3D extracellular matrix composites. Biores Open Access. 2016;5(1):37-48.
17. Darwiche S, Scaletta C, Raffoul W, Pioletti DP, Applegate LA. Epiphyseal chondroprogenitors provide a stable cell source for cartilage cell therapy. Cell Med. 2012;4(1):23-32.
18. Chung R, Foster BK, Xian CJ. Injury responses and repair mechanisms of the injured growth plate. Front Biosci (Schol Ed). 2011;3:117-25.
19. Xian CJ, Bruce FK. Repair of injured articular and growth plate cartilage using mesenchymal stem cells and chondrogenic gene therapy. Curr Stem Cell Res Ther. 2006;1(2):213-29.
20. Xian CJ, Zhou FH, McCarty RC, Foster BK. Intramembranous ossification mechanism for bone bridge formation at the growth plate cartilage injury site. J Orthop Res. 2004;22(2):417-26.
21. Planka L, Gal P, Kecova H, Klima J, Hlucilova J, Filova E, *et al*. Allogeneic and autogenous transplantations of MSCs in treatment of the physeal bone bridge in rabbits. BMC Biotechnol. 2008;8(1):70.
22. Nasu M, Takayama S, Umezawa A: Endochondral ossification model system: designed cell fate of human epiphyseal chondrocytes during long-term implantation. J Cell Physiol. 2015;230(6):1376-88.
23. Walzer SM, Cetin E, Grübl-Barabas R, Sulzbacher I, Rueger B, Girsch W, *et al*. Vascularization of primary and secondary ossification centres in the human growth plate. BMC Dev Biol. 2014;14(1):36.
24. Pichler K, Musumeci G, Vielgut I, Martinelli E, Sadoghi P, Loreto C, *et al*. Towards a better understanding of bone bridge formation in the growth plate–an immunohistochemical approach. Connect Tissue Res. 2013;54(6):408-15.
25. Reinisch A, Bartmann C, Rohde E, Schallmoser K, Bjelic-Radisic V, Lanzer G, *et al*. Humanized system to propagate cord blood-derived multipotent mesenchymal stromal cells for clinical application. Regen Med. 2007;2(4):371-82.
26. Lahm A, Uhl M, Lehr H, Ihling C, Kreuz P, Haberstroh J. Photoshop-based image analysis of canine articular cartilage after subchondral damage. Arch Orthop Trauma Surg. 2004;124(7):431-6.
27. Bustin SA, Beaulieu JF, Huggett J, Jaggi R, Kibenge FS, Olsvik PA, *et al*. MIQE precis: practical implementation of minimum standard guidelines for fluorescence-based quantitative real-time PCR experiments. BMC Mol Biol. 2010;11(1):74.
28. Toegel S, Bieder D, André S, Altmann F, Walzer SM, Kaltner H, *et al*. Glycophenotyping of osteoarthritic cartilage and chondrocytes by RT-qPCR, mass spectrometry, histochemistry with plant/human lectins and lectin localization with a glycoprotein. Arthritis Res Ther. 2013;15(5):R147.
29. Murdoch AD, Grady LM, Ablett MP, Katopodi T, Meadows RS, Hardingham TE. Chondrogenic differentiation of human bone marrow stem cells in transwell cultures: generation of scaffold-free cartilage. *Stem Cells*. 2007;25(11):2786-96.

30. Zeiger AS, Loe FC, Raghunath M, Van Vliet KJ. Influence of altered local effective concentration on cytoskeletal and ECM structure in human mesenchymal stem cells. Biophy J. 2011; 100(3):599a.
31. Li W, Zhu B, Strakova Z, Wang R. Two-way regulation between cells and aligned collagen fibrils: local 3D matrix formation and accelerated neural differentiation of human decidua parietalis placental stem cells. Biochem Biophys Res Commun. 2014;450(4):1377-82.
32. Tummala P, Arnsdorf EJ, Jacobs CR. The role of primary cilia in mesenchymal stem cell differentiation: a pivotal switch in guiding lineage commitment. Cell Mol Bioeng. 2010;3(3):207-12.
33. Yuan X, Yang S. Primary cilia and intraflagellar transport proteins in bone and cartilage. J Dent Res. 2016;95(12):1341-9.
34. Chang CF, Ramaswamy G, Serra R. Depletion of primary cilia in articular chondrocytes results in reduced Gli3 repressor to activator ratio, increased Hedgehog signaling, and symptoms of early osteoarthritis. Osteoarthritis Cartilage. 2012;20(2):152-61.